Chemical Geology 662 (2024) 122220

Contents lists available at ScienceDirect

Chemical Geology

journal homepage: www.elsevier.com/locate/chemgeo

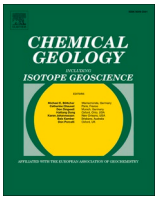

Unravelling instrumental mass fractionation of MC-ICP-MS using neodymium isotopes

Yang Yu [a,b,*], Ed Hathorne [a], Chris Siebert [a], Marcus Gutjahr [a], Jan Fietzke [a], Martin Frank [a]

[a] GEOMAR Helmholtz Centre for Ocean Research, Kiel, Germany
[b] School of Earth and Environmental Sciences, University of St Andrews, St Andrews, United Kingdom

ARTICLE INFO

Editor: Vasileios Mavromatis

Keywords:
Instrumental mass fractionation
Radiogenic Nd isotopes
Stable Nd isotopes
Plasma conditions
Exponential correction
Regression correction
MC-ICP-MS

ABSTRACT

Since the initial discovery of the non-exponential mass fractionation (non-EMF) of Nd isotopes analysis in 2002, similar deviations from an EMF pattern have been reported for measurements of a number of isotope systems (e.g., Si, Ge, Sr, Sn, Ba, Yb, W, Os, Hg and Pb) with MC-ICP-MS. However, the previous controversial reports on the magnitude of the deviations from EMF suggest that instrumental mass bias behaviour of MC-ICP-MS is neither fully understood nor well-characterised. Consequently, the standard approach of using a mass dependent fractionation (MDF) correction model (e.g., exponential law) may lead to both inaccurate and imprecise results. In this study, we systematically characterise the instrumental mass fractionation of MC-ICP-MS using Nd isotope measurements carried out under different plasma conditions, quantified using the normalised argon index (NAI) as an estimate of plasma temperature. Our results indicate that the mass bias of MC-ICP-MS is not always a simple exponential function of mass but shows systematic deviations from an EMF behaviour, which are closely associated with decreased NAIs. As a result, the conventional exponential correction yields a $^{143}Nd/^{144}Nd$ value of 0.512257 for the reference material BHVO-2 when the NAI is low, which is 722 ppm lower than the reported value of 0.512979. By tuning the plasma to higher NAIs (higher plasma temperatures), the deviations from the EMF array are systematically attenuated and the exponential correction is able to correct for the instrumental mass bias under high NAIs. In contrast, a regression correction model for Nd isotopes is developed to account for the observed mass fractionation behaviour that does not follow EMF under low NAIs, given that the regression correction relies on the observed loglinear fractionation of different isotope pairs and does not require both isotope ratios to undergo EMF. We expect that the analytical protocol and fundamental insights gained in this study are applicable to a wide range of other isotope measurements with MC-ICP-MS.

1. Introduction

Multiple-collector inductively coupled plasma mass spectrometry (MC-ICP-MS) has become the method of choice for the fast acquisition of precise and accurate isotope ratio data. The plasma source allows for high ionisation efficiency and a more rapid sample throughput than thermal ionisation mass spectrometry (TIMS). However, MC-ICP-MS displays a large instrumental mass fractionation (bias), typically in the percent range, which is an order of magnitude larger than the characteristic bias observed for TIMS measurements. The mechanisms of this phenomenon are still not fully understood. One concept assumes that the large instrumental mass bias is caused by "space charge effects" in the interface and the focusing lens region (e.g., Jarvis et al., 1992). The high charge density in the ion beam generates electrostatic repulsion between the positively charged ions after they have passed through the skimmer orifice, pushing their trajectories away from the beam axis (e.g., Santos et al., 2007). The degree to which the different isotopes are deflected mainly depends on their respective kinetic energy, which in turn is a function of their mass. While this mechanism would explain some of the effects seen in elemental analyses using ICP-MS instruments, it is currently unclear if "space charge effects" are indeed the primary source of the isotope mass bias in MC-ICP-MS (Rehkämper et al., 2001). In addition, it has been suggested that the large instrumental mass bias is caused by the very high temperature of the plasma, which generates ions with different initial energies and thus with complex trajectories within the mass spectrometer (Albarède et al., 2004). Therefore, correction and compensation of instrumental mass bias and its potential variability is a major concern during MC-ICP-MS measurements and effective

* Corresponding author at: GEOMAR Helmholtz Centre for Ocean Research, Kiel, Germany.
E-mail address: yyu@geomar.de (Y. Yu).

https://doi.org/10.1016/j.chemgeo.2024.122220
Received 24 March 2023; Received in revised form 7 June 2024; Accepted 10 June 2024
Available online 13 June 2024

correction will depend on a thorough understanding of the underlying processes causing mass bias.

A number of correction models for instrumental mass fractionation (e.g., the power and the exponential laws) have been developed and successfully employed for the correction of the mass bias that occurs during TIMS measurements (Russell et al., 1978). However, the current absence of a causal law that accurately describes the mass discrimination of MC-ICP-MS has led to the application of the same correction models as used for TIMS. The exponential law is the most widely applied model to quantify instrumental mass bias for a wide variety of elements. In the case of radiogenic isotope systems (e.g., Nd) which also have stable non-radiogenic isotope pairs, compensation for instrumental mass bias has been realised by internal normalisation, whereby the fractionation factor (β) is determined applying an exponential law using a known non-radiogenic invariant ratio of two Nd masses (e.g., $^{146}Nd/^{144}Nd$). An underlying assumption of exponential correction is that both stable and radiogenic isotope pairs (e.g., $^{146}Nd/^{144}Nd$ and $^{143}Nd/^{144}Nd$) undergo mass dependent fractionation (MDF) following an exponential law. However, it has been observed that this standard approach of using $^{146}Nd/^{144}Nd$ to normalise other Nd isotope ratios (e.g., $^{143}Nd/^{144}Nd$) leads to both inaccurate and imprecise results due to the fact that the observed relationships between measured $^{146}Nd/^{144}Nd$ and $^{143}Nd/^{144}Nd$ are different from that expected for an exponential mass fractionation (EMF, Vance and Thirlwall, 2002). Therefore, the traditional mass bias correction methods, such as the exponential model, may be incapable of adequately correcting for instrumental mass discrimination in MC-ICP-MS.

Previous studies have suggested that observed deviations from normal EMF on MC-ICP-MS are associated with an increased level of Nd oxide formation when a high sensitivity skimmer cone (e.g., "X" cone in the case of Thermo Scientific Neptune Plus) is used (Frères et al., 2021; Newman, 2012; Newman et al., 2009). However, significant departures from EMF have been observed using different skimmer cones (e.g., "H" cone) for Si, Ge, Sr, Sn, Ba, Yb, W, Os, Hg and Pb isotope analysis with MC-ICP-MS (Bragagni et al., 2023; Irrgeher et al., 2013; Shirai and Humayun, 2011; Thirlwall and Anczkiewicz, 2004; Yang et al., 2011, 2018; Zhu et al., 2018). In addition, it is important to note that while the observed instrumental mass bias does not follow the conventional EMF model, it is still mass dependent. Therefore, the term "non-EMF", rather than "mass independent fractionation" (MIF), is used to describe the observed mass bias that deviates from the normal exponential fractionation law in this study.

It has been documented that different combinations of operating conditions (e,g., RF power, gas flows) result in particular thermal conditions of the plasma in the region where it is sampled for isotope analysis (e.g., Fietzke and Frische, 2016). Our research is based on the hypothesis that the variability of the mass bias behaviour of MC-ICP-MS is controlled by different plasma conditions, while the occasional observation of deviations from EMF with specific cone geometry is rather a result of these conditions. Indeed, for a range of elemental analyses with ICP-MS (e.g., Li, B, Fe, Ni, Cu, Sb, Ce, Hf and Re), the magnitude of mass bias was found to be highly affected by the instrumental operating conditions and related processes within the plasma (Andrén et al., 2004; Fontaine et al., 2009). This is further supported by the results of Yu et al. (2020), which demonstrate that different plasma conditions produce significant changes of instrumental mass fractionation for stable Ba isotope analysis with MC-ICP-MS.

To date, only few studies have been devoted to understanding the causal relationship between instrumental mass fractionation and plasma conditions, which is partly due to a large number of interactive instrumental variables and their contributions to different plasma operating states and the difficulty of objectively comparing resulting plasma conditions. In order to better constrain these plasma conditions, Fietzke and Frische (2016) introduced the normalised argon index (NAI) as a quantitative indicator of plasma states:

$$NAI = 2 \cdot {}^{38}Ar^{+} / {}^{40}Ar_2^{+} \quad (1)$$

whereby the $^{38}Ar^{+}$ ion intensity primarily depends on temperature-induced Ar ionisation, while the abundance of $^{40}Ar_2^{+}$ dimer ions decrease with increasing plasma temperature as the Ar-Ar bond is more effectively broken at higher temperature. Normalising the $^{38}Ar^{+}$ to $^{40}Ar_2^{+}$ not only accounts for temperature induced plasma expansion, but also enhances the monitoring sensitivity of plasma temperature. Therefore, the NAI reflects the actual thermal conditions of the plasma at the site of ion sampling regardless of how this state has been achieved by a complex combination of RF power, gas flows and cone geometry (Fietzke and Frische, 2016).

Unlike previous studies that noted instrumental mass bias deviating from the expected EMF occasionally, this study represents a significant advancement by systematically charactering the mass bias behaviour of MC-ICP-MS using the well-known Nd isotope system under a range of quantified plasma conditions (NAI values). It not only confirms previous observations of deviations from EMF but also offers practical guidelines for minimising the magnitude of the observed deviations by increasing NAI values and thereby achieving a simple EMF array. Consequently, the exponential correction is able to resolve the instrumental mass bias during isotope analysis when the NAI is high. Alternatively, a newly developed regression correction method for both radiogenic and stable Nd isotopes is presented to account for the non-EMF behaviours observed under low NAI settings.

2. Instrumental setup

Solutions of the Nd isotopic standard JNdi-1 (Tanaka et al., 2000) and the Nd concentration standard NIST SRM 3135a were used as primary and secondary standards in this study. Note that the NIST SRM 3135a has not been certified for its isotopic composition, which may vary from batch to batch. A basalt rock reference material from the USGS (BHVO-2) was also used in this study. Neodymium was purified using a well-established ion chromatographic technique detailed in previous studies in our lab (cf. Laukert et al., 2017). Briefly, rare earth elements (REEs) were separated from the sample matrix using BioRad AG50W-X8 cation exchange resin following a modified protocol of Münker et al. (2001), followed by a second column with Eichrom Ln-Spec resin to separate Nd from the other REEs following a modified protocol of Pin and Zalduegui (1997).

The Nd isotope data of this study were acquired over approximately two years using a Neptune Plus MC-ICP-MS (Thermo Scientific, Bremen, Germany) in low-resolution mode at GEOMAR, Kiel. The analyte was introduced as a dry aerosol using an Aridus II desolvation system (CETAC Technologies) fitted with an ESI (Elemental Scientific) PFA micro-concentric nebuliser (uptake rate of ~50 µl min^{-1}). Neodymium isotope ratios were measured using either 10 or 50 µg L^{-1} solutions under seven different NAI values. Each plasma state applied during the experiment required the zoom optics, torch positions and source lenses to be tuned for maximum Nd ion transmission. The achieved conditions where then kept constant for the Nd isotope analysis. The NAI values were monitored by measuring mass 38 (i.e. $^{38}Ar^{+}$) and mass 80 (i.e. $^{40}Ar_2^{+}$) under high-resolution mode on the H4 Faraday cup using a 10^{11} Ω resistor at the beginning and the end of each measurement session. It is worth noting that the achieved NAI conditions generally remained stable throughout the measurement sessions. An on-peak zero measurement was conducted by measuring 2% HNO_3 before each sample and applied to the measured Nd signals to account for blank and baseline. The signals of ^{140}Ce and ^{147}Sm were monitored to correct isobaric interferences of ^{142}Ce on ^{142}Nd, ^{144}Sm on ^{144}Nd, ^{148}Sm on ^{148}Nd, and ^{150}Sm on ^{150}Nd. Mass spectrometric precision is given as 2 standard deviations (2SD) of the average $^{143}Nd/^{144}Nd$, $^{142}Nd/^{144}Nd$, and $^{150}Nd/^{144}Nd$ values obtained from repeated analyses of single aliquots.

Previous studies found that the high-sensitivity "X" skimmer cone

geometry is associated with a significantly elevated oxide formation rate, which causes additional contributions to the instrumental mass fractionation (e.g., Newman, 2012). For the experiments of this study, the same "X" skimmer combined with a "Jet" sampler cone were used to show that the instrumental mass bias is not directly linked to a specific cone geometry. Details of instrumental operating parameters and collector configurations are summarised in Table S1.

3. Results and discussion

3.1. Mass fractionation behaviour under different plasma conditions

For the Nd radiogenic isotope system, internal normalisation represents the routine procedure for the elimination of mass discrimination during analysis. The most commonly used correction method for instrumental mass bias is exponential normalisation to $^{146}Nd/^{144}Nd = 0.7219$ (O'Nions et al., 1977). Using the same approach, the corrected $^{143}Nd/^{144}Nd$ ratios of the JNdi-1 standard are plotted for different NAI values in Fig. 1 and Table S2. Note that the benchmark reference value of the $^{143}Nd/^{144}Nd$ ratio used in this study is 0.512107 ± 0.000028, which represents the average of the published values measured by TIMS from the GeoReM database (Jochum et al., 2005). This value is slightly different to the accepted value given by Tanaka et al. (2000) of 0.512115 ± 0.000007.

Our experiments clearly show that the decrease of the NAI (colder plasma) causes systematically larger deviations of the exponentially corrected $^{143}Nd/^{144}Nd$ from the reference value, which become significant when the NAI is below 0.15 (Fig. 1). Amongst those, the lowest tested NAI value of 0.04 results in the maximum deviation of ~600 ppm from the reference value determined by TIMS. By tuning the plasma to a higher NAI (hotter plasma), the deviations of the exponentially corrected $^{143}Nd/^{144}Nd$ ratios from the reference value are systematically attenuated (Fig. 1). This demonstrates that Nd isotope measurements under high NAI are less biased when using the $^{146}Nd/^{144}Nd$ exponential normalisation method. In contrast, the conventionally used exponential correction does not adequately account for the mass discrimination of $^{143}Nd/^{144}Nd$ under low NAI.

Running MC-ICP-MS under a high NAI has been shown to be associated with decreased analyte sensitivity and significantly suppressed oxide formation rate (Fietzke and Frische, 2016; Yu et al., 2020), which for Nd isotope measurements are determined by the voltage of ^{146}Nd per μg L^{-1} and $^{146}NdO/^{146}Nd$ using a pure JNdi-1 standard solution. A negative correlation between analyte sensitivity (Fig. 1), Nd oxide formation rate (Fig. S1) and NAI is observed at the given uptake rate of ~50 μl min^{-1}. Previous studies have suggested that relative analyte sensitivity enhancements and elevated oxide formation rate are caused by different cone geometries (e.g., Newman, 2012; Newman et al., 2009). Our results indicate that significant variations in analyte sensitivity and oxide formation rate can be achieved with the same cone geometries and therefore are likely a function of plasma conditions.

To obtain insights into the underlying mechanisms controlling the mass bias of MC-ICP-MS, we can write the exponential fractionation equations for $^{143}Nd/^{144}Nd$ and $^{146}Nd/^{144}Nd$ as:

$$\left(\frac{^{143}Nd}{^{144}Nd}\right)_{meas} = \left(\frac{^{143}Nd}{^{144}Nd}\right)_{corr} \cdot \left(\frac{M_{143}}{M_{144}}\right)^{\beta_{143/144}} \quad (2)$$

$$\left(\frac{^{146}Nd}{^{144}Nd}\right)_{meas} = \left(\frac{^{146}Nd}{^{144}Nd}\right)_{corr} \cdot \left(\frac{M_{146}}{M_{144}}\right)^{\beta_{146/144}} \quad (3)$$

where the subscripts *meas* and *corr* indicate the measured and mass bias corrected ratios, respectively. M_{143}, M_{144} and M_{146} are the masses of the respective Nd isotopes in amu. The superscripts $\beta_{143/144}$ and $\beta_{146/144}$ refer to the exponential fractionation factors for $^{143}Nd/^{144}Nd$ and $^{146}Nd/^{144}Nd$, respectively. Taking the natural logarithm of Eqs. (2 and 3), we can obtain the relationship between the measured $^{143}Nd/^{144}Nd$ and $^{146}Nd/^{144}Nd$ as:

$$ln\left(\frac{^{143}Nd}{^{144}Nd}\right)_{meas} = ln\left(\frac{^{143}Nd}{^{144}Nd}\right)_{corr} + \frac{\beta_{143/144}}{\beta_{146/144}} \cdot \left[\frac{ln\left(\frac{M_{143}}{M_{144}}\right)}{ln\left(\frac{M_{146}}{M_{144}}\right)}\right] \cdot \left[ln\left(\frac{^{146}Nd}{^{144}Nd}\right)_{meas} - ln\left(\frac{^{146}Nd}{^{144}Nd}\right)_{corr}\right] \quad (4)$$

Accordingly, a logarithmic plot of measured $^{143}Nd/^{144}Nd$ against $^{146}Nd/^{144}Nd$ should yield a straight line with a calculated slope (S_{cal}) of:

$$S_{cal} = \frac{\beta_{143/144}}{\beta_{146/144}} \cdot \left[\frac{ln\left(\frac{M_{143}}{M_{144}}\right)}{ln\left(\frac{M_{146}}{M_{144}}\right)}\right] \quad (5)$$

If the instrumental mass fractionation exclusively corresponds to MDF following the exponential law (i.e. $\beta_{143/144} = \beta_{146/144}$), the predefined slope only depends on Nd masses and the expected gradient for the exponential law is calculated as −0.50 for $^{143}Nd/^{144}Nd$ and $^{146}Nd/^{144}Nd$. However, the observed slopes (S_{obs}) of the best fit lines of

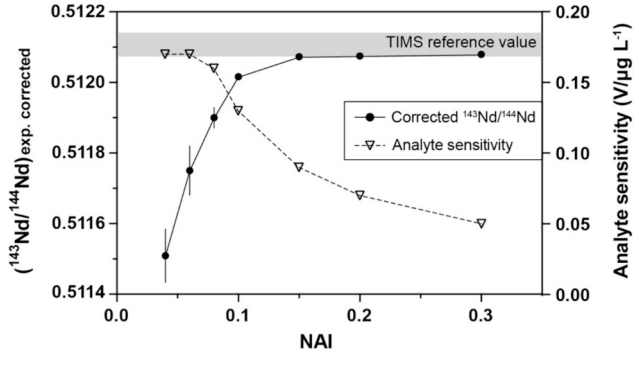

Fig. 1. Exponentially corrected $^{143}Nd/^{144}Nd$ ratios for JNdi-1 standard after normalising to $^{146}Nd/^{144}Nd = 0.7219$ and associated analyte sensitivity against different NAIs. The average values (0.512107 ± 0.000028) obtained by TIMS are given by the shaded band (Jochum et al., 2005). The mean MC-ICP-MS data are 50–600 ppm below the TIMS data. Error bars are given as 2 standard deviations (2SD) of the average $^{143}Nd/^{144}Nd$ value obtained from repeated analyses of single aliquots.

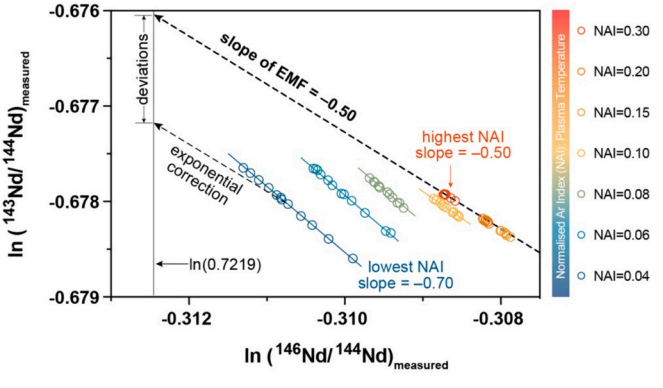

Fig. 2. Plot of the natural logarithm of the measured $^{143}Nd/^{144}Nd$ and $^{146}Nd/^{144}Nd$ for the JNdi-1 standard for different NAI measurement sessions. The observed gradients of the best fit lines of the measured $ln(^{143}Nd/^{144}Nd)$ and $ln(^{146}Nd/^{144}Nd)$ are significantly different from that expected from an exponential mass fractionation (EMF) with a slope of −0.5 when NAI is <0.15. Increasing the NAI gradually shifts the measured raw ratios towards the expected EMF line and for NAIs ≥0.15 they are within error identical.

the measured ln(^{143}Nd/^{144}Nd) and ln(^{146}Nd/^{144}Nd) are clearly different from that expected for an EMF (Fig. 2).

More importantly, lower NAI conditions result in increasing deviations from the expected EMF line, which become significant at NAI values <0.15. Clearly, the data obtained under low NAI do not fall on a line with a slope of −0.50 as predicted by Eq. (5) demonstrating that the assumption $\beta_{143/144} = \beta_{146/144}$ is not valid under inadequate plasma conditions. Given that the exponential mass bias correction (normalised to ^{146}Nd/^{144}Nd = 0.7219) relies on this assumption, it does not provide correct ^{143}Nd/^{144}Nd ratios when the assumption is not fulfilled. Our data clearly show how the exponential correction systematically leads to significant deviations from the reference TIMS value and explain why the exponentially corrected ^{143}Nd/^{144}Nd values vary significantly from session to session. In addition, our experiments confirm that instrumental mass fractionation behaviour is strongly dependent on the plasma state of the MC-ICP-MS and can be rectified.

As shown in Fig. 2, an increase of the NAI gradually shifts the measured raw ratios to the expected EMF line, suggesting that the higher NAIs produce a mass fractionation array that follows an exponential law. Therefore, the exponential correction accounts for the instrumental MDF and yield corrected ^{143}Nd/^{144}Nd values that match the TIMS reference data as shown in Fig. 1. In contrast, the mass discrimination under lower NAIs does not display a simple exponential fractionation dependence on Nd mass. To further investigate the nature of mass fractionation behaviour under low NAIs, a factor Δ is calculated following Vance and Thirlwall (2002) as:

$$\Delta = \frac{\beta_{a/b}}{\beta_{146/144}} \quad (6)$$

where a and b denote different Nd masses. If instrumental mass discrimination is a simple exponential function of mass, then the Δ values should be the same (Δ = 1) across the entire Nd mass range. Fig. 3a shows the β values for the different Nd isotope pairs, normalised to the $\beta_{146/144}$ value and plotted against the numerator Nd masses. A first indication is that the Δ value changes significantly across the limited mass range of Nd, which demonstrates that the $\beta_{146/144}$ value is not the same as other β values for different Nd isotope pairs (e.g., $\beta_{143/144}$) as shown in previous study (Vance and Thirlwall, 2002). A second indication is that the offsets of the β values (i.e. Δ) systematically decrease with increasing NAI but the Δ value is never equal to 1, even under the highest NAI monitored in this experiment (Fig. 3b). This is probably due to the difference of the average mass between ^{143}Nd/^{144}Nd and ^{146}Nd/^{144}Nd (i.e. 143.5 vs 145).

As suggested by Vance and Thirlwall (2002) and Thirlwall and Anczkiewicz (2004), any pair of isotopes with the same average masses should yield a consistent β value. Our results confirm this hypothesis based on two aspects. Firstly, Fig. 3b shows that the $\beta_{143/144}$ is not identical to $\beta_{146/144}$ even under the highest NAI although they are close enough to yield accurate and precise ^{143}Nd/^{144}Nd values as shown in Fig. 1. Secondly, in the case of ^{143}Nd/^{144}Nd, ^{145}Nd/^{142}Nd is the only isotope pair that has the same average mass. As expected, the $\beta_{143/144}$ value is identical to the $\beta_{145/142}$ but this is only the case under high NAIs (Fig. 3b). Similar to the observations of the β value for ^{146}Nd/^{144}Nd, the β offsets between ^{143}Nd/^{144}Nd and ^{145}Nd/^{142}Nd systematically increase with decreasing NAIs (Fig. 3b). This highlights that a high NAI is still necessary to avoid any mass bias that cannot easily be resolved by the widely used exponential mass bias correction.

Generally, running MC-ICP-MS under a low NAI increases the risk of generating instrumental mass bias that does not follow EMF. However, due to the relatively low Nd concentrations in some sample materials (e.g., seawater), a high sensitivity tuning and associated low NAI is unavoidable in some instances. Therefore, for such samples an alternative approach is required to reliably correct for the instrumental mass bias that does not follow a simple EMF law.

3.2. Mass bias correction methods

Given that the exponential correction does not resolve mass bias that does not follow EMF, the commonly applied correction for MC-ICP-MS analyses is the second-order normalisation approach developed by Vance and Thirlwall (2002). In brief, the first-order exponentially corrected ^{143}Nd/^{144}Nd and ^{142}Nd/^{144}Nd ratios were shown to define a tight linear array with a slope between 0.18 and 0.22 that goes through the accepted TIMS values. Therefore, using the relationship defined by the exponentially corrected ^{143}Nd/^{144}Nd and ^{142}Nd/^{144}Nd ratios, the first-order corrected ^{143}Nd/^{144}Nd is additionally normalised to a constant ^{142}Nd/^{144}Nd ratio to account for any residual mass bias effects.

To test the validity of this approach, the exponentially corrected ^{143}Nd/^{144}Nd and ^{142}Nd/^{144}Nd ratios under different NAI values are shown in Fig. 4. It is observed, however, that the best-fit lines do not always pass through the reference TIMS value (e.g., NAI = 0.04 and 0.10), and the slopes of the best-fit lines (0.01–0.41) change significantly between different NAI values. Indeed, Vance and Thirlwall (2002) also noted that the slope of the relationships between the first-order corrected ^{143}Nd/^{144}Nd and ^{142}Nd/^{144}Nd ratios ranges between 0.29 and 0.33 on a Nu MC-ICP-MS instrument, which is clearly different from that observed for their IsoProbe instrument (0.18–0.22). Therefore, checking that the slope between the first-order corrected values fits the predicted value is a necessary test if a second-order correction is appropriate as suggested by Albarède et al. (2004). If this is not the case,

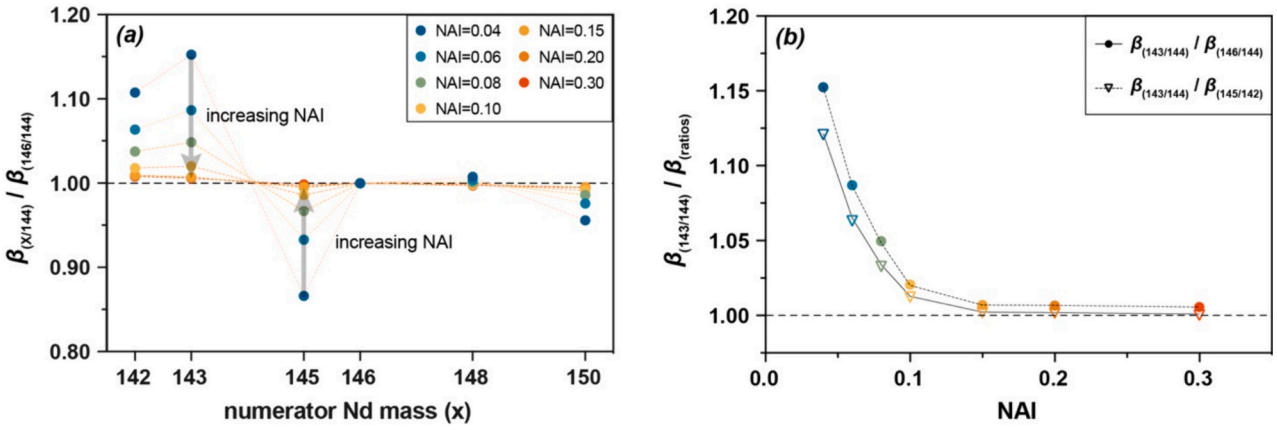

Fig. 3. (a) Variability of exponential fractionation factor β values for the different Nd isotope pairs, normalised to the $\beta_{146/144}$ value and plotted against the numerator Nd mass. (b) Variability of exponential fractionation factor β values for ^{143}Nd/^{144}Nd after normalising to the $\beta_{146/144}$ (solid circles) and $\beta_{145/142}$ (open triangles) and plotted against NAIs.

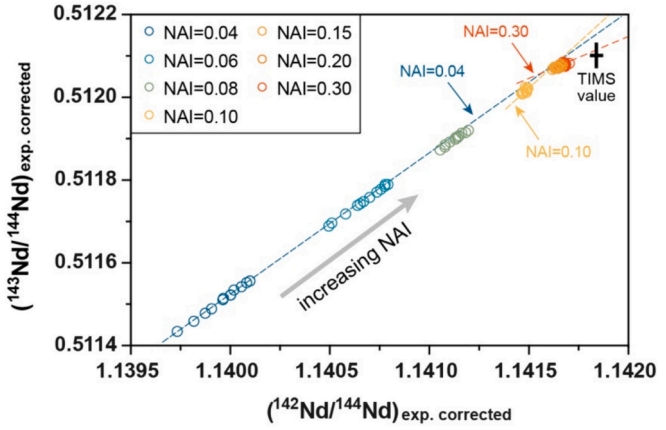

Fig. 4. Plot of exponentially corrected $^{143}Nd/^{144}Nd$ and $^{142}Nd/^{144}Nd$ ratios after normalising to $^{146}Nd/^{144}Nd = 0.7219$ (O'Nions et al., 1977) under different NAIs. The best-fit lines of exponentially corrected $^{143}Nd/^{144}Nd$ and $^{142}Nd/^{144}Nd$ do not always pass through the accepted TIMS values (black cross, Jochum et al., 2005) and the slope of the best-fit line changes significantly between different NAIs (e.g., NAI = 0.04, 0.10 and 0.30).

we suggest a different approach, a regression correction, to account for the instrumental mass bias of Nd isotope measurements.

As shown in section 3.1, the measured ln($^{143}Nd/^{144}Nd$) and ln ($^{146}Nd/^{144}Nd$) do not fit the EMF line under low NAI and thus the β values for $^{143}Nd/^{144}Nd$ and $^{146}Nd/^{144}Nd$ are different (Eq. (5)). However, as long as the ratio of $\beta_{143/144}$ and $\beta_{146/144}$ remains constant (i.e. Δ is constant but not 1), a plot of measured $^{143}Nd/^{144}Nd$ and $^{146}Nd/^{144}Nd$ should still form a straight line in ln-ln Nd isotope space. Indeed, our Nd isotope results demonstrate that the ratio of $\beta_{143/144}$ and $\beta_{146/144}$ stays constant over the course of an analytical session under the same NAI. Therefore, an empirical relationship between $\beta_{143/144}$ and $\beta_{146/144}$ can be defined, whereby the slope (S_{obs}) can be directly obtained by the logarithmic plot of measured $^{143}Nd/^{144}Nd$ and $^{146}Nd/^{144}Nd$ (Fig. 5). Given that the alignment of the measured ln($^{143}Nd/^{144}Nd$) and ln ($^{146}Nd/^{144}Nd$) is tight ($R^2 = 0.99$), we can obtain the corrected $^{143}Nd/^{144}Nd$ ratios as:

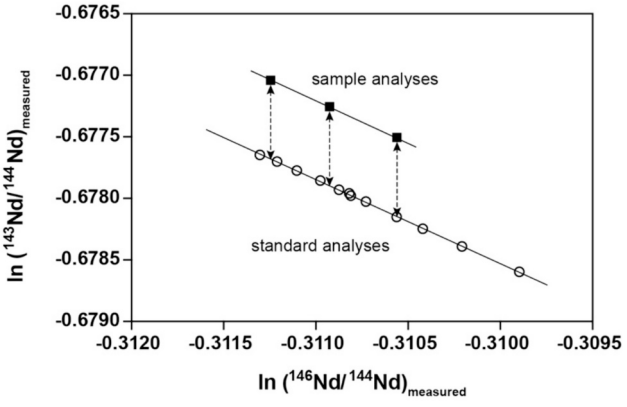

Fig. 5. Principle of the regression correction for Nd isotopes. The slope of the regression line (S_{obs}) is determined by analysing the JNdi-1 Nd standard (open circles). The difference between a particular sample (solid squares) and a standard is equal to the vertical distance between the regression lines drawn through the data points representing the sample and the standard and with the same slope.

$$ln\left(\frac{^{143}Nd}{^{144}Nd}\right)_{corr} = ln\left(\frac{^{143}Nd}{^{144}Nd}\right)_{std} + ln\left(\frac{^{143}Nd}{^{144}Nd}\right)_{smp} - S_{obs}\cdot ln\left(\frac{^{143}Nd}{^{144}Nd}\right)_{smp} + \Phi\cdot\frac{ln\left(\frac{^{143}Nd}{^{144}Nd}\right)_{std}}{ln\left(\frac{^{146}Nd}{^{144}Nd}\right)_{std}} \quad (7)$$

where Φ and S_{obs} are the intercept and the slope of the best estimates of the measured ln($^{143}Nd/^{144}Nd$) and ln($^{146}Nd/^{144}Nd$) array for a set of standard runs (e.g., JNdi-1) over a period of time overlapping with that of the sample measurements. The subscripts *std* and *smp* denote standard and sample, respectively. As shown in Fig. 5, the difference between the logarithm of the measured ratios for samples and standards is simply the vertical distance between the parallel lines with the slope (S_{obs}) being defined by the standard runs. Given that the principle of this approach was initially developed by Maréchal et al. (1999) for correcting stable Cu and Zn isotope measurements by MC-ICP-MS, the stable isotope pairs of Nd (e.g., $^{142}Nd/^{144}Nd$ and $^{150}Nd/^{144}Nd$) are also assessed by this regression correction method.

The single-stage corrected $^{143}Nd/^{144}Nd$, $^{142}Nd/^{144}Nd$, and $^{150}Nd/^{144}Nd$ and associated reproducibility of the secondary standard NIST SRM 3135a using regression correction (open squares) and exponential normalisation (solid circles) are shown in Fig. 6 and Table S2. Clearly, the $^{146}Nd/^{144}Nd$ exponential normalisation results in both significantly inaccurate and imprecise Nd isotope ratios under a relatively low NAI (Fig. 6, solid circles). This is because the measured raw ratios do not display a EMF and thus cannot be accurately and precisely corrected by the exponential fractionation law. In contrast, the regression correction yields consistent $^{143}Nd/^{144}Nd$, $^{142}Nd/^{144}Nd$, and $^{150}Nd/^{144}Nd$ values with good precisions that are independent from NAI (Fig. 6, open squares). This is because the regression correction relies on the observed loglinear fractionation of different isotope pairs and does not require both isotope ratios to undergo EMF.

The accuracy and reproducibility of this regression correction method were further tested by including a large set of NIST SRM 3135a data obtained in our lab over approximately two years, during which measurements were not monitored for NAI but were likely carried out under different day to day plasma conditions. The mass bias corrected $^{143}Nd/^{144}Nd$ ratios by two different correction models are illustrated in Fig. 7. Clearly, the single-stage exponential correction yields an average value of 0.512398 ± 0.000014 (2SD, $n = 149$), which shows large deviations from the reported value of 0.512449 ± 0.000010 (Huang et al., 2020). In comparison, the single-stage regression correction greatly improves the long-term reproducibility and yields an average value of 0.512450 ± 0.000005 (2SD, n = 149), which is consistent with the reported value of 0.512449 ± 0.000010 (Huang et al., 2020). This long-term precision of the regression correction is generally comparable with the reproducibility of approximately 0.000010 achieved with TIMS measurements, which is significantly lower than the variability of $^{143}Nd/^{144}Nd$ in natural samples.

One of the underlying assumptions of the regression correction is that the loglinear relationship between two isotope ratios is well-defined. Previous studies have suggested that by addition of matrix elements to analyte solutions, a large spread in mass bias can be artificially generated on MC-ICP-MS and thus define mass bias relationships between element pairs more precisely (Archer and Vance, 2004; Woodhead, 2002). Given that the magnitude of mass bias is a function of NAI, the instrumental mass fractionation is normally large thus allowing the calculation of a regression with low uncertainty when NAI is low as shown in Fig. 2. Therefore, the empirical slope can be precisely defined without doping with matrix elements and estimating the slope does not introduce a significant error in the corrected ratios. In addition, another underlying assumption of the regression correction is that the slope remains constant between sample and standard analyses, the likelihood of

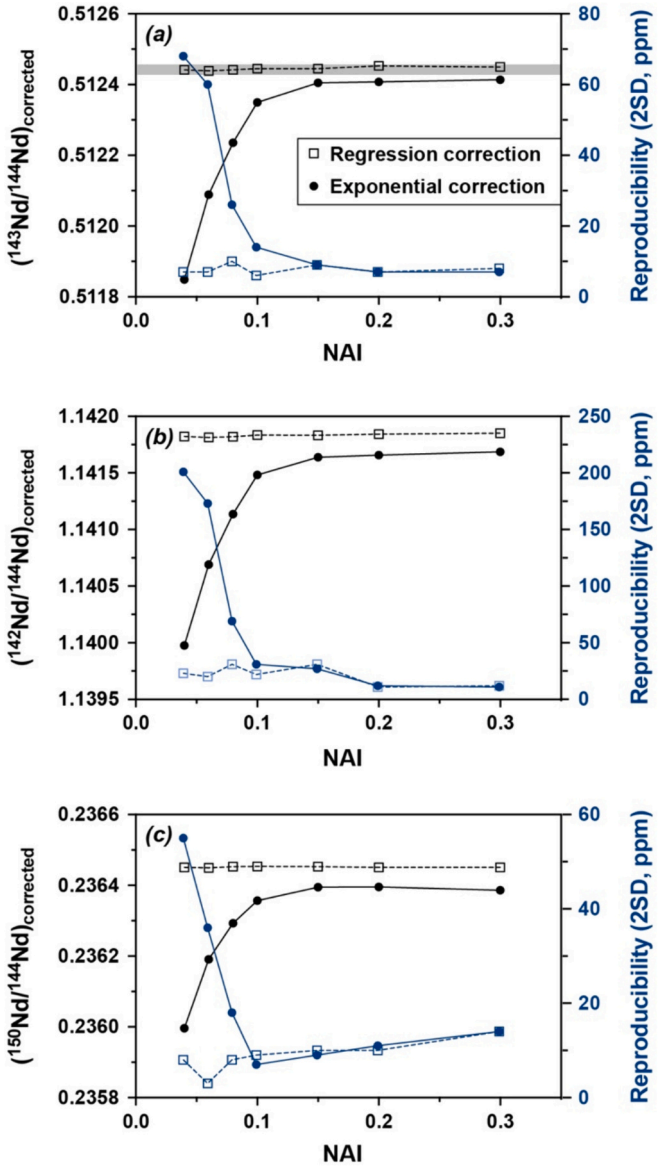

Fig. 6. The instrumental mass bias corrected (a) $^{143}Nd/^{144}Nd$ ratios, (b) $^{142}Nd/^{144}Nd$ ratios, (c) $^{150}Nd/^{144}Nd$ ratios, and associated reproducibility of the secondary standard NIST SRM 3135a using the regression correction (open squares) and exponential correction (solid circles) under different NAIs. The reported value of 0.512449 ± 0.000010 for $^{143}Nd/^{144}Nd$ ratio (Huang et al., 2020) is given by the shaded band.

which is higher if purification of the sample has been efficient. Given the first order aim to minimise Ce and Sm interferences prior to measurement, an efficient purification of Nd is still necessary when conducting a regression correction approach under low NAIs.

3.3. Nd isotope compositions of reference material BHVO-2

To verify the proposed analytical protocol with two different correction approaches, the USGS basalt reference material BHVO-2 has been analysed under low and high NAI conditions. Analyte Nd concentrations of 10 μg L^{-1} and 50 μg L^{-1} were measured under a low NAI of 0.05 and a high NAI of 0.26, respectively. Both exponential and regression correction methods were applied for mass bias correction during each session. All corrected $^{143}Nd/^{144}Nd$, $^{142}Nd/^{144}Nd$, and $^{150}Nd/^{144}Nd$ ratios are shown in Table 1. When NAI is 0.05, the single-stage exponential correction yields an average value of 0.512257 ± 0.000031, 1.139621 ± 0.000098, and 0.235948 ± 0.000070 for $^{143}Nd/^{144}Nd$, $^{142}Nd/^{144}Nd$, and $^{150}Nd/^{144}Nd$, respectively, which are significantly lower than the reported value compiled by the GeoReM database (Jochum et al., 2005). In contrast, using the same exponential correction method under high NAI yields average values of 0.512963 ± 0.000004, 1.141748 ± 0.000013, and 0.236346 ± 0.000005 for $^{143}Nd/^{144}Nd$, $^{142}Nd/^{144}Nd$, and $^{150}Nd/^{144}Nd$, respectively, which agree well with the reported value. In comparison, the regression correction yields average values of $^{143}Nd/^{144}Nd$ = 0.512993 ± 0.000017, $^{142}Nd/^{144}Nd$ = 1.141864 ± 0.000059, and $^{150}Nd/^{144}Nd$ = 0.236467 ± 0.000036 at NAI of 0.05, which are comparable with the regression corrected Nd isotope ratios ($^{143}Nd/^{144}Nd$ = 0.512982 ± 0.000009, $^{142}Nd/^{144}Nd$ = 1.141849 ± 0.000016, and $^{150}Nd/^{144}Nd$ = 0.236454 ± 0.000005) at NAI of 0.26. All the corrected Nd isotope ratios obtained from regression corrections show good agreement with the values reported in the literature (Jochum et al., 2005). The slightly worse reproducibility of regression correction under an NAI of 0.05 is mainly a consequence of the lower analyte Nd concentration (10 μg L^{-1}) and associated worse statistics.

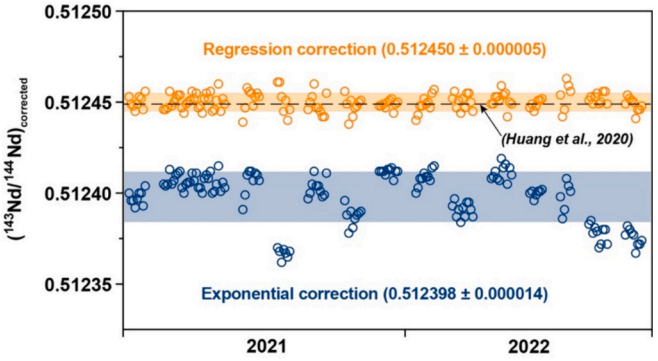

Fig. 7. The instrumental mass bias corrected $^{143}Nd/^{144}Nd$ ratios of the secondary standard NIST SRM 3135a using the regression correction (orange) and exponential correction (blue) from different measurement sessions over approximately two years. The reported value of 0.512449 (Huang et al., 2020) is given by the dash line. (For interpretation of the references to colour in this figure legend, the reader is referred to the web version of this article.)

In brief, we suggest that the regression correction method can be used for radiogenic and stable isotope pairs under a range of NAI defined plasma conditions and is especially suitable for low Nd concentration analysis (e.g., <10 μg L^{-1}) with significantly enhanced Nd sensitivity and associated low NAI. The clear offsets in the exponentially corrected $^{143}Nd/^{144}Nd$, $^{142}Nd/^{144}Nd$, and $^{150}Nd/^{144}Nd$ ratios obtained under a low NAI indicate that the widely used exponential correction method for radiogenic Nd isotopes should only be applied under high NAI conditions.

4. Conclusions

A systematic investigation of instrumental mass fractionation of MC-ICP-MS has been carried out using neodymium (Nd) isotopes under a range of plasma conditions (NAI). When the NAI is low, the exponentially corrected $^{143}Nd/^{144}Nd$ values for JNdi-1 standard show significant deviations from the accepted value determined by TIMS. This is because the instrumental mass bias of isotope analysis does not match the exponential mass fractionation (EMF) model. In contrast, the magnitude of the deviations from EMF array can be systematically attenuated by increasing NAI. Thereby the exponential correction is able to resolve the mass bias during isotope analysis when NAI is high. Alternatively, a regression correction method is presented to account for the observed mass fractionation behaviour that does not follow EMF under a low NAI. This is because the regression correction relies on the observed loglinear fractionation of different isotope pairs and does not require both isotope

Table 1
The instrumental mass bias corrected $^{143}Nd/^{144}Nd$, $^{142}Nd/^{144}Nd$ and $^{150}Nd/^{144}Nd$ ratios of reference material BHVO-2 using the exponential correction and regression correction under NAI of 0.05 and 0.26. The reported Nd isotope values for BHVO-2 are from GeoReM database (Jochum et al., 2005).

BHVO-2		GeoReM	Exponential Correction		Regression Correction	
		database	NAI = 0.05 10 μg L^{-1} Nd	NAI = 0.26 50 μg L^{-1} Nd	NAI = 0.05 10 μg L^{-1} Nd	NAI = 0.26 50 μg L^{-1} Nd
$^{143}Nd/^{144}Nd$	AVE	0.512979	0.512257	0.512963	0.512993	0.512982
	2SD	0.000023	0.000031	0.000004	0.000017	0.000009
	n	85	3	4	3	4
$^{142}Nd/^{144}Nd$	AVE	1.141836	1.139621	1.141748	1.141864	1.141849
	2SD	0.000005	0.000098	0.000013	0.000059	0.000016
	n	6	3	4	3	4
$^{150}Nd/^{144}Nd$	AVE	0.236456	0.235948	0.236346	0.236467	0.236454
	2SD	0.000012	0.000070	0.000005	0.000036	0.000005
	n	6	3	4	3	4

ratios to undergo EMF. The accuracy and precision of our suggested approach for both radiogenic and stable Nd isotope analysis are further verified by analyses of the secondary standard NIST SRM 3135a and a well-studied reference material (BHVO-2) with two different correction approaches under low and high NAIs. The Nd isotope ratios of NIST SRM 3135a and BHVO-2 obtained from the exponential correction under high NAI conditions show good agreement with corrected values from regression corrections under both high and low NAI and the previously reported Nd isotope values. The large offsets of exponentially corrected Nd isotope values obtained under low NAI indicate that the commonly used exponential correction can only be applied under high NAI conditions. We expect that our proposed approach will also enable an improved determination of other isotope systems with MC-ICP-MS.

CRediT authorship contribution statement

Yang Yu: Conceptualization, Formal analysis, Investigation, Methodology, Visualization, Writing – original draft, Writing – review & editing. **Ed Hathorne:** Writing – review & editing, Funding acquisition. **Chris Siebert:** Writing – review & editing. **Marcus Gutjahr:** Writing – review & editing. **Jan Fietzke:** Methodology, Writing – review & editing. **Martin Frank:** Funding acquisition, Project administration, Writing – review & editing.

Declaration of competing interest

The authors declare that they have no known competing financial interests or personal relationships that could have appeared to influence the work reported in this paper.

Data availability

Data will be made available on request.

Acknowledgement

The Deutsche Forschungsgemeinschaft (DFG, German Research Foundation) – Project number 468592241 (M.F.) – SPP 2299/Project number 441832482 is acknowledged for financial support of Y. Y. during this study. We thank Dr. Julien T. Middleton, Prof. Matthew Thirlwall and one anonymous reviewer for their insightful comments. Dr. Vasileios Mavromatis is acknowledged for his efficient editorial handling.

Appendix A. Supplementary data

Supplementary data to this article can be found online at https://doi.org/10.1016/j.chemgeo.2024.122220.

References

Albarède, F., Telouk, P., Blichert-Toft, J., Boyet, M., Agranier, A., Nelson, B., 2004. Precise and accurate isotopic measurements using multiple-collector ICPMS. Geochim. Cosmochim. Acta 68, 2725–2744. https://doi.org/10.1016/j.gca.2003.11.024.

Andrén, H., Rodushkin, I., Stenberg, A., Malinovsky, D., Baxter, D.C., 2004. Sources of mass bias and isotope ratio variation in multi-collector ICP-MS: optimization of instrumental parameters based on experimental observations. J. Anal. At. Spectrom. 19, 1217–1224. https://doi.org/10.1039/B403938F.

Archer, C., Vance, D., 2004. Mass discrimination correction in multiple-collector plasma source mass spectrometry: an example using Cu and Zn isotopes. J. Anal. At. Spectrom. 19, 656. https://doi.org/10.1039/b315853e.

Bragagni, A., Wombacher, F., Kirchenbaur, M., Braukmüller, N., Münker, C., 2023. Mass-independent Sn isotope fractionation and radiogenic 115Sn in chondrites and terrestrial rocks. Geochim. Cosmochim. Acta 344, 40–58. https://doi.org/10.1016/j.gca.2023.01.014.

Fietzke, J., Frische, M., 2016. Experimental evaluation of elemental behavior during LA-ICP-MS: influences of plasma conditions and limits of plasma robustness. J. Anal. At. Spectrom. 31, 234–244. https://doi.org/10.1039/C5JA00253B.

Fontaine, G.H., Hattendorf, B., Bourdon, B., Günther, D., 2009. Effects of operating conditions and matrix on mass bias in MC-ICPMS. J. Anal. At. Spectrom. 24, 637. https://doi.org/10.1039/b816948a.

Frères, E., Weis, D., Newman, K., Amini, M., Gordon, K., 2021. Oxide Formation and Instrumental Mass Bias in MC-ICP-MS: an Isotopic Case Study of Neodymium. Geostand. Geoanal. Res. 45, 501–523. https://doi.org/10.1111/ggr.12381.

Huang, H., Gutjahr, M., Eisenhauer, A., Kuhn, G., 2020. No detectable Weddell Sea Antarctic Bottom Water export during the last and Penultimate Glacial Maximum. Nat. Commun. 11, 424. https://doi.org/10.1038/s41467-020-14302-3.

Irrgeher, J., Prohaska, T., Sturgeon, E., Mester, R.Z., Yang, L., 2013. Determination of strontium isotope amount ratios in biological tissues using MC-ICPMS. Anal. Methods 5, 1687–1694. https://doi.org/10.1039/C3AY00028A.

Jarvis, K.E., Gray, A.L., Houk, R.S., Jarvis, I., McLaren, J.W., Williams, J.G., 1992. Handbook of Inductively Coupled Plasma Mass Spectrometry.

Jochum, K.P., Nohl, U., Herwig, K., Lammel, E., Stoll, B., Hofmann, A.W., 2005. GeoReM: a New Geochemical Database for Reference Materials and Isotopic Standards. Geostand. Geoanal. Res. 29, 333–338. https://doi.org/10.1111/j.1751-908X.2005.tb00904.x.

Laukert, G., Frank, M., Bauch, D., Hathorne, E.C., Gutjahr, M., Janout, M., Hölemann, J., 2017. Transport and transformation of riverine neodymium isotope and rare earth element signatures in high latitude estuaries: a case study from the Laptev Sea. Earth Planet. Sci. Lett. 477, 205–217. https://doi.org/10.1016/j.epsl.2017.08.010.

Maréchal, C.N., Télouk, P., Albarède, F., 1999. Precise analysis of copper and zinc isotopic compositions by plasma-source mass spectrometry. Chem. Geol. 156, 251–273. https://doi.org/10.1016/S0009-2541(98)00191-0.

Münker, C., Weyer, S., Scherer, E., Mezger, K., 2001. Separation of high field strength elements (Nb, Ta, Zr, Hf) and Lu from rock samples for MC-ICPMS measurements. Geochem. Geophys. Geosyst. 2 https://doi.org/10.1029/2001GC000183.

Newman, K., 2012. Effects of the sampling interface in MC-ICP-MS: Relative elemental sensitivities and non-linear mass dependent fractionation of Nd isotopes. J. Anal. At. Spectrom. 27, 63–70. https://doi.org/10.1039/C1JA10222B.

Newman, K., Freedman, P.A., Williams, J., Belshaw, N.S., Halliday, A.N., 2009. High sensitivity skimmers and non-linear mass dependent fractionation in ICP-MS. J. Anal. At. Spectrom. 24, 742. https://doi.org/10.1039/b819065h.

O'nions, R.K., Hamilton, P.J., Evensen, N.M., 1977. Variations in143Nd/144Nd and87Sr/86Sr ratios in oceanic basalts. Earth Planet. Sci. Lett. 34, 13–22.

Pin, C., Zalduegui, J.S., 1997. Sequential separation of light rare-earth elements, thorium and uranium by miniaturized extraction chromatography: Application to isotopic analyses of silicate rocks. Anal. Chim. Acta 339, 79–89. https://doi.org/10.1016/S0003-2670(96)00499-0.

Rehkämper, M., Schönbächler, M., Stirling, C.H., 2001. Multiple Collector ICP-MS: Introduction to Instrumentation, Measurement Techniques and Analytical Capabilities. Geostand. Geoanal. Res. 25, 23–40. https://doi.org/10.1111/j.1751-908X.2001.tb00785.x.

Russell, W.A., Papanastassiou, D.A., Tombrello, T.A., 1978. Ca isotope fractionation on the Earth and other solar system materials. Geochim. Cosmochim. Acta 42, 1075–1090. https://doi.org/10.1016/0016-7037(78)90105-9.

Santos, R., Canto Machado, M.J., Ruiz, I., Sato, K., Vasconcelos, M.T.S.D., 2007. Space charge and mass discrimination effects on lead isotope ratio measurements by ICP-QMS in environmental samples with high uranium content. J. Anal. At. Spectrom. 22, 783. https://doi.org/10.1039/b618783h.

Shirai, N., Humayun, M., 2011. Mass independent bias in W isotopes in MC-ICP-MS instruments. J. Anal. At. Spectrom. 26, 1414. https://doi.org/10.1039/c0ja00206b.

Tanaka, T., Togashi, S., Kamioka, H., Amakawa, H., Kagami, H., Hamamoto, T., Yuhara, M., Orihashi, Y., Yoneda, S., Shimizu, H., Kunimaru, T., Takahashi, K., Yanagi, T., Nakano, T., Fujimaki, H., Shinjo, R., Asahara, Y., Tanimizu, M., Dragusanu, C., 2000. JNdi-1: a neodymium isotopic reference in consistency with LaJolla neodymium. Chem. Geol. 168, 279–281. https://doi.org/10.1016/S0009-2541(00)00198-4.

Thirlwall, M.F., Anczkiewicz, R., 2004. Multidynamic isotope ratio analysis using MC–ICP–MS and the causes of secular drift in Hf, Nd and Pb isotope ratios. Int. J. Mass Spectrom. 235 (1), 59–81.

Vance, D., Thirlwall, M., 2002. An assessment of mass discrimination in MC-ICPMS using Nd isotopes. Chem. Geol. 185, 227–240. https://doi.org/10.1016/S0009-2541(01)00402-8.

Woodhead, J., 2002. A simple method for obtaining highly accurate Pb isotope data by MC-ICP-MS. J. Anal. At. Spectrom. 17, 1381–1385.

Yang, L., Mester, Z., Zhou, L., Gao, S., Sturgeon, R.E., Meija, J., 2011. Observations of large Mass-Independent Fractionation Occurring in MC-ICPMS: Implications for Determination of Accurate Isotope Amount Ratios. Anal. Chem. 83, 8999–9004. https://doi.org/10.1021/ac201795v.

Yang, L., Tong, S., Zhou, L., Hu, Z., Mester, Z., Meija, J., 2018. A critical review on isotopic fractionation correction methods for accurate isotope amount ratio measurements by MC-ICP-MS. J. Anal. At. Spectrom. 33 (11), 1849–1861.

Yu, Y., Siebert, C., Fietzke, J., Goepfert, T., Hathorne, E., Cao, Z., Frank, M., 2020. The impact of MC-ICP-MS plasma conditions on the accuracy and precision of stable isotope measurements evaluated for barium isotopes. Chem. Geol. 549, 119697 https://doi.org/10.1016/j.chemgeo.2020.119697.

Zhu, Z., Meija, J., Tong, S., Zheng, A., Zhou, L., Yang, L., 2018. Determination of the Isotopic Composition of Osmium using MC-ICPMS. Anal. Chem. 90, 9281–9288. https://doi.org/10.1021/acs.analchem.8b01859.